

# Measurements of Saturation Densities in the Critical Region of Pentafluoroethyl Methyl Ether (245cbE $\beta\gamma$ )<sup>†</sup>

Yasutaka Yoshii,<sup>\*,‡</sup> Masao Mizukawa,<sup>‡</sup> Januarius V. Widiatmo,<sup>‡,§</sup> and Koichi Watanabe<sup>‡</sup>

Department of System Design Engineering, Faculty of Science and Technology, Keio University, 3-14-1, Hiyoshi, Kohoku-ku, Yokohama 223-8522, Japan

We have measured 10 saturated-vapor densities and 13 saturated-liquid densities in the critical region of pentafluoroethyl methyl ether, CF<sub>3</sub>CF<sub>2</sub>OCH<sub>3</sub> (245cbE $\beta\gamma$ ), based on the direct visual observation of the meniscus disappearance in an optical cell. The critical temperature and density have been determined by taking into consideration the meniscus disappearing level of the sample within the optical cell as well as the intensity of the critical opalescence. The experimental uncertainties of saturation temperature and density measurements were estimated to be within  $\pm 12$  mK and  $\pm(0.5$  to  $4.0)$  kg·m<sup>-3</sup>, while those of the critical temperature and density values determined are to be within  $\pm 17$  mK and  $\pm 3$  kg·m<sup>-3</sup>, respectively. We have also determined the critical exponent,  $\beta$ , and the critical amplitude,  $B$ , on the basis of the vapor–liquid coexistence curve correlation developed.

## Introduction

The Research Institute of Innovative Technology for the Earth (RITE), Kyoto, Japan, has issued a challenge to synthesize several candidates as long-term alternatives among fluorinated ethers under the Development of New Refrigerant, Blowing Agent and Cleaning Solvent for Effective Use of Energy Project.<sup>1</sup> The compounds proposed have the possibility to be the new-generation alternative refrigerants, because of their zero ODP values and negligible GWP values. One of the most promising fluorinated ethers, pentafluoroethylmethylether, CF<sub>3</sub>CF<sub>2</sub>OCH<sub>3</sub> (245cbE $\beta\gamma$ ), could be a replacement for dichlorotetrafluoroethane, CClF<sub>2</sub>–CClF<sub>2</sub> (R-114), especially for high-temperature vapor-compression heat pump applications. However, reliable experimental information about the thermodynamic properties of this substance is still very limited even for the critical parameters that are important in predicting various thermodynamic properties and in formulating equations of state.

This paper reports measurements of the saturation densities in the critical region, and the determined critical temperature and density values. In addition, we have also developed a vapor–liquid coexistence curve correlation from which the critical exponent,  $\beta$ , and the critical amplitude,  $B$ , have been determined.

## Experimental Section

The saturation densities in the vicinity of the critical point were measured by means of direct observation of the meniscus (vapor–liquid coexistence interface) disappearance and critical opalescence. A phenomenon involving a fluid becoming colored dark brown or black in the vicinity of the critical point is known as the critical opalescence,

since only the light with longer wavelength can penetrate the sample fluid which would be composed of molecular clusters near the critical point. In addition to the critical opalescence, we have also paid full attention to the level at which the meniscus disappeared.

Special caution was paid to establish a uniform temperature field for a certain period of time in order to maintain a well-established thermal equilibrium condition. When the average sample density in the optical cell is greater than the critical density, the sample meniscus locates just a little higher than the middle of the optical cell and critical opalescence becomes intense in the liquid phase. When it is smaller than the critical density, on the other hand, the meniscus locates just a little lower than the middle of the optical cell and critical opalescence becomes intense in the vapor phase. The temperature at which the sample meniscus disappears is regarded as the saturation temperature corresponding to the average sample fluid density. By repeating these measurements along different isochores in the vicinity of the critical point, it becomes feasible to determine the critical temperature and critical density rather precisely with small uncertainties.

The experimental apparatus used for the present measurements was originally reported by Okazaki et al.,<sup>2</sup> and Tanikawa et al.<sup>3</sup> made some modifications. Since then, a series of similar measurements have been completed with respect to HCFC and HFC refrigerants and their mixtures including R-23,<sup>2</sup> R-123,<sup>3</sup> R-236ea,<sup>4</sup> R-143a,<sup>4</sup> R-134a,<sup>4</sup> R-125 + R-134a,<sup>5</sup> and R-32 + R-143a.<sup>5</sup>

Figure 1 shows the schematic of the experimental apparatus. The apparatus consists of three vessels: an optical cylindrical cell (A) with two synthetic sapphire windows at both ends for observing the meniscus of the sample refrigerant, an expansion vessel (B) for making expansion, and a supplying vessel (C) for supplying the sample refrigerant. The inner volumes of the optical cell, the expansion vessel, and the supplying vessel are (11.108  $\pm$  0.006) cm<sup>3</sup>, (6.297  $\pm$  0.007) cm<sup>3</sup>, and (77.457  $\pm$  0.009) cm<sup>3</sup>, respectively. These three vessels are made of stainless steel, and all are installed on a horizontal frame that can

\* To whom correspondence should be addressed. Fax: +81-45-566-1720. E-mail: yoshii@ws.sd.keio.ac.jp.

<sup>†</sup> This contribution will be part of a special print edition containing papers presented at the Fourteenth Symposium on Thermophysical Properties, Boulder, CO, June 25–30, 2000.

<sup>‡</sup> Keio University.

<sup>§</sup> Permanent Researcher at Agency for the Assessment and Application of Technology, Jl. M. H. Thamrin No. 8, Jakarta 10340, Indonesia.

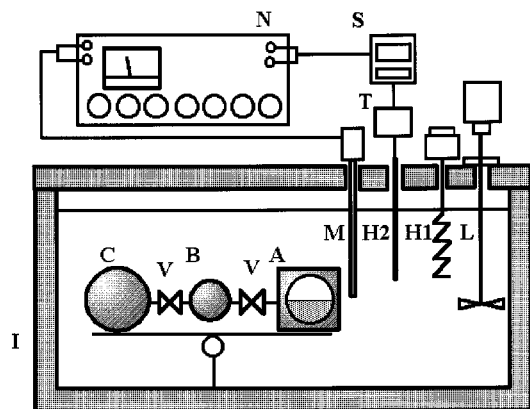


**Figure 1.** Experimental apparatus: A, optical cell; B, expansion vessel; C, supplying vessel; H1, main heater; H2, subheater; I, thermostated bath; L, stirrer; M, platinum resistance thermometer; N, thermomometer bridge; S, PID controller; T, voltage converter; V, valves.

be rocked. This assembly is set in a thermostated fluid bath (I) where silicone oil is filled and circulated by a stirrer (L). Since the cylindrical optical cell (A) is considered to be a constant-volume cell in principle, the known mass of the sample confined in the optical cell has to be expanded into the expansion cell (B) at a prescribed temperature in the single-phase region. The rocking device mentioned above is effective at maintaining the densities in three vessels unchanged before and after the sample expansion.

Temperature is measured with a  $25\ \Omega$  standard platinum resistance thermometer (M) calibrated against ITS-90, and it is installed near the optical cell in the thermostated fluid bath (I). Special caution was paid to establish a uniform temperature for a certain period of time in order to maintain the well-established thermal equilibrium condition. To keep the temperature constant, this standard platinum resistance thermometer detects the temperature fluctuation and then the temperature of the thermostated bath fluid is maintained by the PID controller (S) within  $\pm 2$  mK over several hours. Therefore, we believe the sample temperature is equal to the bath fluid temperature when the thermal equilibrium has been well established.

We have evaluated the experimental uncertainties on the basis of the ISO recommendation<sup>6</sup> associated with a coverage factor of 2. The expanded uncertainty of the saturation density measurements varies from  $\pm(0.5$  to  $4.0)$   $\text{kg}\cdot\text{m}^{-3}$ , whereas that of the saturation temperature is  $\pm 12$  mK.

The purity of the sample used for the measurements is 99.9967 mol % for  $\text{CF}_3\text{CF}_2\text{OCH}_3$ , according to the analysis made by the RITE. The sample has been furnished by the RITE, and no further purification has been applied in the present study.

## Results

Concerning  $\text{CF}_3\text{CF}_2\text{OCH}_3$ , 10 saturated-vapor density data points and 13 saturated-liquid density data points have been obtained in the critical region. The experimental results are given in Table 1, where  $\rho''$  denotes the saturated-vapor density and  $\rho'$  the saturated-liquid density. The uncertainty of the temperature measurements depends on the fluctuation of the thermostated bath temperature, the reliability of the thermometer, and the individual error with respect to the determination of the meniscus-disappearing temperature. The uncertainty of the temperature

**Table 1.** Saturated-Vapor and -Liquid Densities of  $245\text{cbE}\beta\gamma$

$\rho''/\text{kg}\cdot\text{m}^{-3}$	$T/\text{K}$	$\rho'/\text{kg}\cdot\text{m}^{-3}$	$T/\text{K}$
$324.9 \pm 0.7$	404.708	$509.9 \pm 0.5^a$	406.834
$348.8 \pm 2.2$	405.629	$510.1 \pm 3.2^a$	406.829
$365.8 \pm 2.7$	405.984	$515.5 \pm 1.9^a$	406.814
$373.5 \pm 1.4$	406.125	$542.0 \pm 0.6^a$	406.819
$400.1 \pm 0.5$	406.465	$546.3 \pm 2.0^a$	406.799
$441.1 \pm 4.0$	406.769	$552.2 \pm 0.6^a$	406.774
$449.4 \pm 4.0^a$	406.809	$573.1 \pm 3.6^a$	406.723
$472.4 \pm 3.0^a$	406.804	$585.2 \pm 0.6^a$	406.612
$481.3 \pm 3.0^a$	406.809	$590.6 \pm 3.7^a$	406.592
$506.0 \pm 1.9^a$	406.824	604.9 $\pm$ 0.6	406.500
		613.9 $\pm$ 2.2	406.323
		632.6 $\pm$ 2.3	405.994
		657.5 $\pm$ 0.6	405.487

<sup>a</sup> Density values obtained when the critical opalescence was observed.

measurements is estimated to be within  $\pm 12$  mK. The uncertainty of the density measurements depends on the number of expansion procedures and varies from  $\pm(0.5$  to  $4.0)$   $\text{kg}\cdot\text{m}^{-3}$ , as shown in Table 1. Figure 2 summarizes the present results on a temperature–density diagram together with the saturation densities measured by Tsuge et al.<sup>7</sup>

The critical opalescence was observed at 13 measurements for the densities between  $(449.4$  and  $590.6)$   $\text{kg}\cdot\text{m}^{-3}$ . These measurements are given with an asterisk for the measured density values in Table 1. For eight saturated-vapor densities below  $472.4$   $\text{kg}\cdot\text{m}^{-3}$  the meniscus descended with increasing temperature and disappeared at the bottom of the optical cell. For nine saturated-liquid densities above  $546.3$   $\text{kg}\cdot\text{m}^{-3}$ , the meniscus ascended with increasing temperature and it disappeared at the top of the optical cell. At the other six density values near the critical density, the meniscus disappeared without reaching either the top or bottom of the optical cell.

At the density of  $506.0$   $\text{kg}\cdot\text{m}^{-3}$ , the critical opalescence in the liquid phase was observed more intensely than that in the vapor phase. At this density the meniscus descended slightly before it disappeared. As a whole, the most intense critical opalescence was observed at the density  $509.9$   $\text{kg}\cdot\text{m}^{-3}$ , where the critical opalescence in the vapor phase was a little more intense than that in the liquid phase. At this density the meniscus ascended slightly before it disappeared. On the basis of these observations, we considered that the density  $509.9$   $\text{kg}\cdot\text{m}^{-3}$  was the saturated-liquid density but the closest density to the critical point among the present results. Therefore, the critical density should be between these two density values, and we determined it to be  $\rho_c = (509 \pm 3)$   $\text{kg}\cdot\text{m}^{-3}$ .

The critical temperature can be determined as the saturation temperature that corresponds to the critical density. As shown in Table 1, the temperature range and the density range between  $(506.0$  and  $510.1)$   $\text{kg}\cdot\text{m}^{-3}$  are in good agreement with each other within the uncertainty of the temperature measurements. Therefore, we determined the critical temperature to be  $T_c = (406.830 \pm 0.017)$  K.

## Discussion

For the critical density and temperature, the comparison between the present results and the literature values reported by Sako et al.<sup>8</sup> is presented in Table 2. The present critical temperature value agrees with the value reported by Sako et al.<sup>8</sup> within the mutual estimated uncertainties. The critical density reported by Sako et al.<sup>8</sup> is lower than

**Table 2. Comparison of the Critical Temperature and Density**

ref	$T_c$ /K	$\rho_c$ /kg·m <sup>-3</sup>	sample purity/mol %
Sako et al. <sup>8</sup>	406.80 ± 0.03	499 ± 1	99.9
this work	406.830 ± 0.017	509 ± 3	99.9967

**Table 3. Numerical Constants in Eq 2**

$D_0$	$D_1$	$D_2$	$B_0$	$B_1$
-7.653 38	13.3526	-7.412 79	1.959 50	-0.384 531

our measurement by 10 kg·m<sup>-3</sup>. The critical density value reported by Sako et al.<sup>8</sup> was exclusively obtained by their measurement at the critical point. On the other hand, we have performed our measurements over and over in the vicinity of the critical point, and the critical density was determined by a careful examination of the measured saturated-vapor and -liquid densities, which are extremely close to the critical point. Besides, the purity of the sample by Sako et al.<sup>8</sup> was 99.9 mol %, while we used the sample with the purity of 99.9967 mol %. Therefore, we believe our results would be fairly reliable.

The critical exponent,  $\beta$ , is used to represent the vapor–liquid coexistence curve in the critical region by means of the following power-law representation:

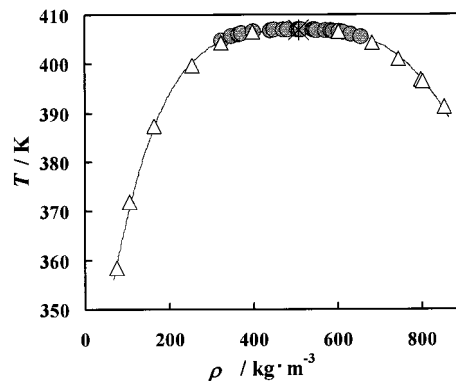
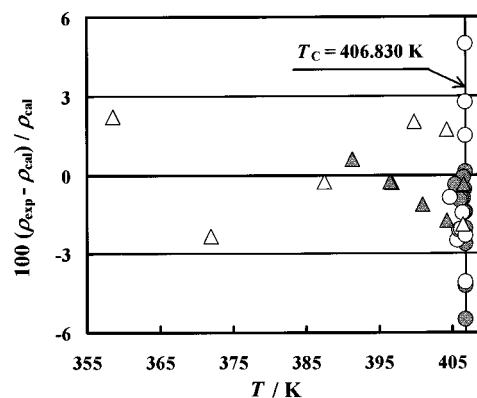
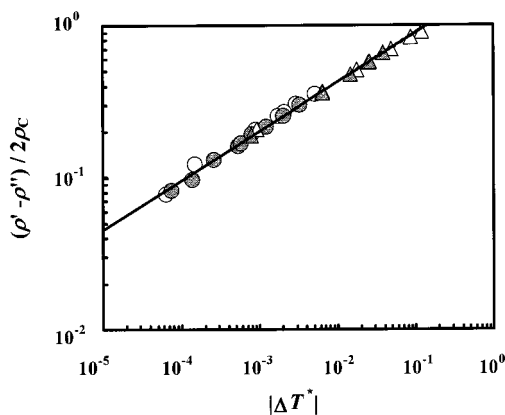
$$(\rho' - \rho'')/2\rho_c = B[(T_c - T)/T_c]^\beta \quad (1)$$

where  $\rho_c$  is the critical density,  $T_c$  is the critical temperature, single and double primes denote the saturated-vapor and -liquid phases, respectively, and  $B$  is the critical amplitude. Equation 1 requires isothermal pairs of liquid and vapor density values. Therefore, we used the following correlation for the calculation of the corresponding saturated-vapor and -liquid densities:

$$\Delta\rho^* = D_0|\Delta T^*|^{(1-\alpha)} + D_1|\Delta T^*| + D_2|\Delta T^*|^{(1-\alpha+\Delta_1)} \pm B_0|\Delta T^*|^\beta \pm B_1|\Delta T^*|^{(\beta+\Delta_1)} \quad (2)$$

where  $\Delta\rho^* = (\rho - \rho_c)/\rho_c$ ,  $|\Delta T^*| = (T_c - T)/T_c$ ,  $\alpha$  and  $\beta$  are the critical exponents, and  $T$  is the temperature in Kelvin. The exponent  $\Delta_1$  stands for the first symmetric correction-to-scaling exponent of the Wegner expansion.<sup>9</sup> From the theoretical background of eq 2, these exponents are  $\alpha = 0.1085$ ,  $\beta = 0.325$ , and  $\Delta_1 = 0.50$ .<sup>9</sup> The critical parameters in eq 2 are those determined in this study, being  $T_c = 406.830$  K and  $\rho_c = 509$  kg·m<sup>-3</sup>. On the basis of the present measurements and available saturation density data reported by Tsuge et al.,<sup>7</sup> the coefficients  $D_0$ ,  $D_1$ ,  $D_2$ ,  $B_0$ , and  $B_1$  in eq 2 were determined by the least-squares fitting, as summarized in Table 3. In this least-squares fitting, we have used 28 data points including 16 present data points and 12 data points by Tsuge et al.<sup>7</sup> as a set of input data, by excluding 7 present measurements in the very vicinity of the critical point corresponding to  $|\Delta T^*| < 6.0 \times 10^{-5}$ . The upper sign “+” and the lower sign “-” of the fourth and fifth terms in eq 2 correspond to the saturated-liquid and -vapor phase, respectively. Equation 2 is effective for the range of densities between (75.0 and 854.2) kg·m<sup>-3</sup>. The vapor–liquid coexistence curve calculated from eq 2 is shown in Figure 2. The density deviations of the present measurements and the measurements reported by Tsuge et al.<sup>7</sup> from eq 2 are illustrated in Figure 3. Equation 2 reproduces the input data among the present measurements and the measurements reported by Tsuge et al.<sup>7</sup> within  $\pm 2.3\%$  in density.

Figure 4 shows a logarithmic plot between  $(\rho' - \rho'')/2\rho_c$  and  $|\Delta T^*|$  in terms of the present measurements and

**Figure 2.** Vapor–liquid coexistence curve of CF<sub>3</sub>CF<sub>2</sub>OCH<sub>3</sub>: ●, this work; △, Tsuge et al.; \*, critical point.**Figure 3.** Density deviation from eq 2: ○, this work (saturated vapor density); ●, this work (saturated liquid density); △, Tsuge et al.<sup>7</sup> (saturated vapor density); ▲, Tsuge et al.<sup>7</sup> (saturated liquid density).**Figure 4.** Critical exponent and amplitude: ○, this work (saturated vapor density); ●, this work (saturated liquid density); △, Tsuge et al.<sup>7</sup> (saturated vapor density); ▲, Tsuge et al.<sup>7</sup> (saturated liquid density);  $\beta = 0.324$ ;  $B = 1.89$ .

calculated results from eq 2. The power-law representation, eq 1, suggests that a straight line can fit the experimental results satisfactorily. The slope of the straight line is equivalent to the critical exponent,  $\beta$ . For the determination of the critical exponent,  $\beta$ , and the critical amplitude,  $B$ , we used the data utilized for determination of the coefficients in eq 2. As a result of the least-squares fitting, the values of  $\beta$  and  $B$  were obtained, being  $\beta = 0.324$  and  $B = 1.89$ . The  $\beta$  value is close to the theoretical value of 0.325.<sup>9</sup>

## Conclusions

By means of visual observation of the meniscus in the optical cell, 10 saturated-vapor densities and 13 saturated-

liquid densities of pentafluoroethyl methyl ether in the critical region were measured, and the critical density, critical temperature, critical exponent, and critical amplitude were determined. Saturated vapor–liquid density correlation for this fluorinated ether was also developed on the basis of the present measurements.

### Acknowledgment

We are grateful to the RITE for furnishing the research-grade samples.

### Literature Cited

- (1) Sekiya, A.; Misaki, S.; A Continuing Search for New Refrigerants. *Chemtech* **1996**, *26*, 44–48.
- (2) Okazaki, S.; Higashi, Y.; Takaishi, Y.; Uematsu, U.; Watanabe, K. Procedures for Determining the Critical Parameters of Fluids. *Rev. Sci. Instrum.* **1983**, *54*, 21–25.
- (3) Tanikawa, S.; Kabata, Y.; Sato, H.; Watanabe, K. Measurements of the Critical Parameters and the Vapor-Liquid Coexistence Curve in the Critical Region of HCFC-123. *J. Chem. Eng. Data* **1990**, *35*, 381–385.
- (4) Aoyama, H.; Kishizawa, G.; Sato, H.; Watanabe, K. Vapor-Liquid Coexistence Curves in the Critical Region and the Critical Temperatures and Densities of 1,1,1,2-Tetrafluoroethane (R-134a), 1,1,1-Trifluoroethane (143a), and 1,1,1,2,3,3-Hexafluoropropane (R-236ea). *J. Chem. Eng. Data* **1996**, *41*, 1046–1051.
- (5) Kishizawa, G.; Sato, H.; Watanabe, K. Measurements of Saturation Densities in Critical Region and Critical Loci for Binary R32/125 and R-125/143a Systems. *Int. J. Thermophys.* **1999**, *20*, 923–932.
- (6) International Organization for Standardization. *Guide to the Expression of Uncertainty in Measurement*; ISO: Switzerland, 1993.
- (7) Tsuge, T.; Sato, H.; Watanabe, K. Vapor Pressure and PVT Properties of HFE-245mc (pentafluoroethyl methyl ether). *Rev. High Pressure Sci. Technol.* **1998**, *7*, 1198–1200.
- (8) Sako, T.; Sato, M.; Nakazawa, N.; Oowa, M.; Yasumoto, M.; Ito, H.; Yamashita, S. Critical Properties of Fluorinated Ethers. *J. Chem. Eng. Data* **1996**, *41*, 802–805.
- (9) Levelt Sengers, J. M. H.; Sengers, J. V. In *Perspectives in Statistical Physics*; Raveche, H. J., Ed.; North-Holland: Amsterdam, 1981; Chapter 14.

Received for review August 4, 2000. Accepted December 20, 2000. The present study was partially supported by the New Energy and Industrial Technology Development Organization (NEDO), Tokyo, Japan, through the RITE.

JE000252F